© 2016. Published by The Company of Biologists Ltd | Journal of Cell Science (2016) 129, 3583-3596 doi:10.1242/jcs.190074

RESEARCH ARTICLE

The polarity protein Scribble positions DLC3 at adherens junctions to regulate Rho signaling

Janina Hendrick[1], Mirita Franz-Wachtel[2], Yvonne Moeller[1], Simone Schmid[1], Boris Macek[2] and Monilola A. Olayioye[1,*]

ABSTRACT

The spatial regulation of cellular Rho signaling by GAP proteins is still poorly understood. By performing mass spectrometry, we here identify the polarity protein Scribble as a scaffold for the RhoGAP protein DLC3 (also known as StarD8) at cell–cell adhesions. This mutually dependent interaction is mediated by the PDZ domains of Scribble and a PDZ ligand (PDZL) motif in DLC3. Both Scribble depletion and PDZL deletion abrogated DLC3 junctional localization. Using a RhoA biosensor and a targeted GAP domain, we demonstrate that DLC3 activity locally regulates RhoA–ROCK signaling at and Scribble localization to adherens junctions, and is required for their functional integrity. In a 3D model of cyst development, we furthermore show that DLC3 depletion impairs polarized morphogenesis, phenocopying the effects observed upon Scribble knockdown. We thus propose a new function for Scribble in Rho regulation that entails positioning of DLC3 GAP activity at cell junctions in polarized epithelial cells.

KEY WORDS: Apical-basolateral polarity, Adherens junctions, Rho GTPase-activating protein, PDZ domain interaction, Tumor suppressor

INTRODUCTION

The establishment and maintenance of apical-basal cell polarity is essential for the normal function and integrity of highly organized epithelia. In polarized epithelial cells, proteins and lipids are asymmetrically distributed between an apical membrane compartment defined by the Par and Crumbs complexes and a basolateral membrane domain characterized by the Scribble complex (Halaoui and McCaffrey, 2015; Iden and Collard, 2008). Adherens junctions mediate strong cell–cell adhesions, whereas tight junctions act as permeability barriers to maintain the asymmetric distribution of molecules and the spatial organization of signaling pathways. Loss of polarity occurs at an early stage of epithelial cancers. Thus, understanding of the molecular mechanisms that regulate epithelial cell polarity will provide deeper insights into the different steps of tumor progression (Ellenbroek et al., 2012; Halaoui and McCaffrey, 2015).

In *Drosophila*, the Scribble (Scrib) polarity protein, together with Discs large (Dlg) and Lethal giant larvae (Lgl), is required for the maintenance of apical-basolateral polarity, whereas in mammalian cells the dominant function of Scribble appears to be within the planar polarity pathway (Humbert et al., 2008; Montcouquiol et al., 2003; Murdoch et al., 2003). Scribble acts as a tumor suppressor in *Drosophila* and mammalian cells, and its loss cooperates with oncogenic Ras signaling in cell transformation (Bilder and Perrimon, 2000; Dow et al., 2003, 2008; Pagliarini and Xu, 2003). Scribble is a multidomain scaffold protein containing 16 leucine-rich repeats (LRRs) and four PSD-95, ZO-1 and Discs large (PDZ) domains as platforms for protein–protein interactions (Albertson et al., 2004; Humbert et al., 2008). Loss of Scribble expression has been reported in breast and colorectal cancer, and is associated with disrupted epithelial cell polarity and disorganized tissue architecture including abnormal E-cadherin localization (Gardiol et al., 2006; Navarro et al., 2005). This can be explained in part by the role of Scribble in stabilizing the interaction of E-cadherin and p120-catenin at adherens junctions (Lohia et al., 2012). The correct membrane localization of Scribble is essential for its functions because mislocalized Scribble impairs polarized morphogenesis and fails to inhibit Ras-induced cell invasion of MCF10A breast epithelial cells (Elsum and Humbert, 2013; Zhan et al., 2008).

Cell polarization requires spatially restricted cytoskeleton remodeling, which is mediated by the cooperation of polarity proteins and small GTPases of the Rho family (Iden and Collard, 2008; Ngok et al., 2014). Rho GTPases, including RhoA, Rac and Cdc42 as the best-characterized members, function as key regulators of actin and microtubule dynamics and are involved in the control of cell polarity, adhesion and migration (Jaffe and Hall, 2005). Rho proteins act as binary switches cycling between an active GTP-bound and an inactive GDP-bound state. This is regulated by guanine nucleotide exchange factors (GEFs), which promote the exchange of GDP for GTP to activate the GTPase and induce signaling of downstream effectors. GTPase-activating proteins (GAPs) enhance the intrinsic GTPase activity of the Rho proteins, returning them into the inactive form (Bos et al., 2007; Vigil et al., 2010).

The establishment of antagonistic Rac and RhoA activity gradients along the apical-basal axis is required for junction formation and maturation (Mack and Georgiou, 2014). Rac activation, for example, is controlled by the GEF protein Tiam, which itself is activated by the basolateral scaffold β2-Syntrophin and inhibited by apical Par3 (Mack et al., 2012; Mertens et al., 2005; Nishimura et al., 2005). Scribble contributes to spatially controlled Rho activation by targeting β-Pix (also known as ARHGEF7), a GEF for Rac and Cdc42 to adherens junctions to form a signaling complex with PAK2 regulating normal epithelial morphogenesis (Frank et al., 2012). Moreover, the Scribble–β-Pix complex controls the activation of PAK proteins and Rac at the leading edge of migrating cells (Nola et al., 2008). During the maturation of adherens junctions, active Rac promotes the association of p190RhoGAPa (ARHGAP35) with cadherin-bound

[1]Institute of Cell Biology and Immunology, University of Stuttgart, Allmandring 31, Stuttgart 70569, Germany. [2]Proteome Center Tübingen, University of Tübingen, Auf der Morgenstelle 15, Tübingen 72076, Germany.

*Author for correspondence (monilola.olayioye@izi.uni-stuttgart.de)

M.A.O., 0000-0003-1093-263X

Received 31 March 2016; Accepted 1 August 2016

Journal of Cell Science (2016) 129, 3583-3596 doi:10.1242/jcs.190074

p120-catenin, thereby suppressing RhoA activation (Noren et al., 2003; Wildenberg et al., 2006). However, studies using FRET biosensors have revealed that RhoA is active in the periphery of contacting cells during the initial phase of cell–cell adhesion (Yamada and Nelson, 2007). Recently, p114RhoGEF (also known as ARHGEF18) was identified as the first junction-associated regulator of Rho signaling at the apical membrane regulating junction assembly and epithelial morphogenesis (Terry et al., 2011), whereas the RhoGEF Ect2 is recruited to zonula adherens to control RhoA-mediated actomyosin dynamics and junction integrity (Ratheesh et al., 2012).

The RhoGAP protein deleted in liver cancer 3 (DLC3), also known as StarD8, is a still poorly characterized member of the DLC family that is downregulated in different types of cancer (Durkin et al., 2007a,b). Similar to DLC1 and DLC2 (also known as StarD13), DLC3 contains an N-terminal sterile α motif (SAM), a C-terminal steroidogenic acute regulatory protein-related lipid transfer (START) domain and a GAP domain that regulates RhoA activity (Braun and Olayioye, 2015; Durkin et al., 2007b; Kawai et al., 2007). In addition to the association with focal adhesions that is common to all DLC isoforms, we have previously reported DLC3 localization to cell–cell contacts and Rab8-positive membranes tubules (Braun et al., 2015; Holeiter et al., 2012; Qian et al., 2007). Given that the focal-adhesion-associated tensin and talin adaptors are the only known DLC3-interacting proteins identified thus far (Li et al., 2011; Qian et al., 2007), it is unclear how DLC3 is recruited to distinct subcellular sites to execute its functions. Here, we identify Scribble as a DLC3-specific binding partner that positions the protein through a unique C-terminal PDZ ligand motif at cell junctions. Our studies provide evidence that DLC3 recruitment is crucial for spatially balanced RhoA–ROCK signaling at adherens junctions and the polarized morphogenesis of epithelial cells in 3D culture.

RESULTS

DLC3 interacts with the basolateral polarity protein Scribble

To identify molecular factors that specify DLC3 localization, we performed mass spectrometry analysis of DLC3-interacting proteins. Flag-tagged wild-type (WT) DLC3 and a DLC3 point mutant (K725E) previously shown to be GAP inactive (Holeiter et al., 2012) were transiently expressed in HEK293T cells and immunopurified from cell lysates, followed by analysis of the samples by nano-liquid chromatography tandem mass spectrometry (nanoLC-MS/MS). For each detected co-immunoprecipitating protein, semi-quantitative intensity-based absolute quantification (iBAQ) values were calculated (see Materials and Methods for details). To exclude the bulk of non-specific binders, we set an arbitrary iBAQ threshold of ≥100,000 and considered only the highest scoring proteins that associated with DLC3 WT and K725E but that were not present in the empty vector control. This analysis yielded 228 proteins (Table S1). In accordance with the role of DLC3 in transferrin receptor trafficking to the endocytic membrane compartment (Braun et al., 2015), several proteins involved in membrane trafficking, including the early endosome marker Rab5 and the transferrin receptor (TfnR) were contained in the list of interacting proteins (Table S1). Interestingly, 17 proteins were associated with the category ‘cell junction’ as based on GOCC annotation (Table 1). We noted that seven of these proteins contain PDZ domains, which are prominent protein interaction platforms. These PDZ domain proteins included Scribble, Dlg1, GOPC, Lin-7 and α1-, β1- and β2-syntrophin (Table 1). We focused our biological follow-up on the polarity protein Scribble because it localizes to adherens junctions and the basolateral membrane of polarized epithelial cells, and functions as a potential tumor suppressor (Dow et al., 2003; Navarro et al., 2005; Qin et al., 2005).

Table 1. Cell-junction-associated DLC3-binding partners according to GOCC annotation

Protein name(s)	Symbol	PDZ domain
Protein scribble homolog	SCRIB	+
Disks large homolog 1	DLG1	+
Golgi-associated PDZ and coiled-coil motif-containing protein	GOPC	+
Protein lin-7 homolog C, A or B	LIN7C; LIN7A; LIN7B	+
Alpha-1-syntrophin	SNTA1	+
Beta-1-syntrophin	SNTB1	+
Beta-2-syntrophin	SNTB2	+
Angiomotin-like protein 2	AMOTL2	–
Cyclin-dependent kinase 4	CDK4	–
Cytochrome c1, heme protein, mitochondrial	CYC1	–
DnaJ homolog subfamily A member 3, mitochondrial	DNAJA3	–
Dystrobrevin alpha	DTNA	–
Dystrobrevin; Dystrobrevin beta	DTNB	–
BTB/POZ domain-containing protein KCTD12	KCTD12	–
Obscurin-like protein 1	OBSL1	–
Plakophilin-2	PKP2	–
Utrophin	UTRN	–

To first validate the interaction of DLC3 and Scribble biochemically, GFP–Scribble was transiently expressed in HEK293T cells, immunoprecipitated from cell lysates with an anti-GFP antibody and binding of co-expressed Flag-tagged DLC3 was confirmed by immunoblotting (Fig. 1A). In agreement with the mass spectrometry analysis, WT and GAP-inactive DLC3 were bound by Scribble with comparable affinity, indicating that the interaction occurs independently of the GAP activity of DLC3 (Fig. S1). We confirmed the interaction of endogenous DLC3 and Scribble by co-immunoprecipitation of the proteins from HeLa cell lysates using a DLC3-specific antibody (Fig. 1B). Considering the structural similarity of the three DLC proteins, we asked whether Scribble also interacts with DLC1 and DLC2. In Scribble immunoprecipitates, coexpressed DLC1 and DLC2 were not detectable even in long exposures (Fig. 1C and data not shown), indicating predominant interaction with the DLC3 isoform. Scribble contains four PDZ domains (Humbert et al., 2008) that often mediate protein interactions with C-terminal PDZ ligand (PDZL) motifs (x-S/T-x-L/V) (Nourry et al., 2003). Intriguingly, DLC3 contains such a C-terminal PDZL motif (ETKL) that is absent in DLC1 and DLC2 (Fig. 1D). To prove a direct PDZ-domain-mediated interaction of Scribble with DLC3, we generated DLC3 ΔPDZL, a deletion mutant lacking the five C-terminal amino acids, and analyzed binding by far western blotting. To this end, Flag-tagged full-length DLC3 and DLC3 ΔPDZL were expressed in HEK293T cells, enriched by immunoprecipitation and transferred to membrane. Membranes were then incubated with a recombinant Scribble protein fragment encompassing the PDZ domains (GST–Scribble-PDZ1-PDZ4) or GST alone. Immunostaining revealed that the PDZ domains of Scribble bound to the full-length DLC3 protein, whereas deletion of the PDZL motif abrogated Scribble binding (Fig. 1D). Thus, we can conclude that the interaction of DLC3 and Scribble is direct and mediated by the PDZ domains of Scribble and the C-terminal PDZL

Journal of Cell Science (2016) 129, 3583-3596 doi:10.1242/jcs.190074

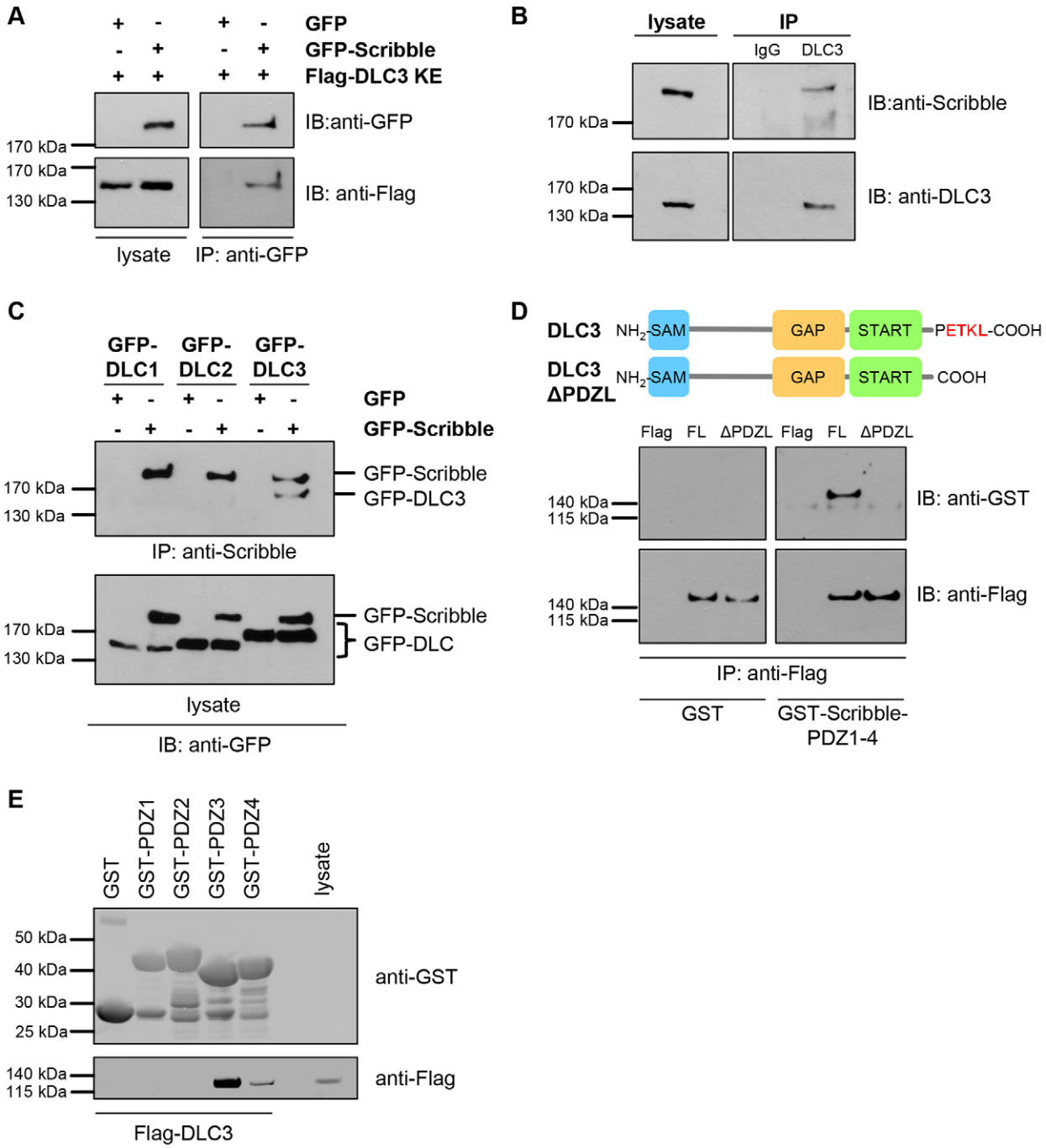

Fig. 1. DLC3 directly interacts with Scribble via a C-terminal PDZ ligand motif. (A) HEK293T cells were transfected with expression vectors encoding GFP–Scribble or GFP alone along with Flag–DLC3 K725E, respectively. The next day, lysates were immunoprecipitated (IP) with an anti-GFP antibody. Samples were analyzed by immunoblotting (IB) using anti-GFP and anti-Flag antibodies. (B) Endogenous DLC3 was immunoprecipitated from HeLa cell lysates and co-immunoprecipitation of endogenous Scribble was analyzed by immunoblotting. An unrelated IgG was used as a control. (C) HEK293T cells were transfected with expression vectors encoding GFP–Scribble or GFP alone and GFP–DLC1, GFP–DLC2 or GFP–DLC3, respectively. At 24 h post transfection, cell lysates were immunoprecipitated with Scribble-specific antibody and analyzed by immunoblotting using anti-GFP antibody. (D) Domain organization of human DLC3 and DLC3 ΔPDZL lacking the last five amino acids (PETKL). SAM, sterile alpha motif; START, steroidogenic acute regulatory protein-related lipid transfer domain. HEK293T cells were transfected with plasmids encoding Flag–DLC3 full-length (FL), Flag–DLC3 ΔPDZL or empty Flag vector. At 24 h post transfection, Flag–DLC3 proteins were immunoprecipitated from lysates and subjected to immunoblotting. For far western blotting, membranes were incubated with recombinant GST–Scribble PDZ1–PDZ4 or GST (control) and stained with GST- and Flag-specific antibodies. (E) Pulldown of Flag–DLC3 transiently expressed in HEK293T cells with glutathione beads coupled to GST–Scribble PDZ1, PDZ2, PDZ3 or PDZ4 or GST alone. Bound proteins were analyzed by immunoblotting with anti-GST and anti-Flag antibodies.

motif of DLC3. Finally, to determine which of the four Scribble PDZ domains was involved in DLC3 binding, we performed pulldown experiments of DLC3 with immobilized GST-tagged Scribble PDZ1, PDZ2, PDZ3 or PDZ4. Immunoblotting showed that DLC3 was primarily bound by Scribble PDZ3 and to a lesser extent by Scribble PDZ4 (Fig. 1E).

Journal of Cell Science (2016) 129, 3583-3596 doi:10.1242/jcs.190074

Junctional DLC3 localization is specified by its PDZ ligand motif and Scribble

We next sought to visualize the interaction of DLC3 and Scribble at the cellular level by performing an *in situ* proximity ligation assay (PLA). These studies were performed in MCF7 cells stably expressing GFP–DLC3 because DLC3-specific antibodies are not suited for the detection of the endogenous protein by immunofluorescence. Because cell morphology is not perturbed by GAP-inactive DLC3, cells expressing DLC3 K725E were preferably used for the colocalization studies with endogenous Scribble. Indeed, the proximity ligation reaction led to the accumulation of discrete fluorescent spots at cell adhesions, whereas almost no signal was observed in the control without primary antibodies and only weak background signals were seen in cells lacking GFP–DLC3 expression (Fig. 2A). The significant increase of the junctional PLA signal compared to the controls confirms specificity and proves the *in situ* interaction of DLC3 and Scribble at cell–cell contacts (Fig. 2B).

To next investigate whether DLC3 localization depends on Scribble, we transfected MCF7 cells stably expressing DLC3 with non-targeting (spNT) or Scribble-specific (spScrib) small interfering RNAs (siRNAs) and immunostained the cells 3 days post transfection. In control cells, DLC3 strongly colocalized with E-cadherin at cell–cell adhesions. However, upon Scribble depletion, both DLC3 WT and K725E no longer accumulated at cell–cell contacts and were homogeneously distributed within the cell (Fig. 3A; Fig. S2A). Although adherens junctions were less ordered in cells lacking Scribble, junctional E-cadherin localization was partially retained, whereas DLC3 was completely mislocalized from cell–cell contacts, as confirmed by a significantly reduced Mander's colocalization coefficient in the knockdown cells (Fig. 3B). Efficient downregulation of Scribble was verified by immunoblotting (Fig. 3C) and independent siRNAs targeting Scribble yielded similar results, ruling out off-target effects (Fig. S2B,C). These findings strongly suggest that DLC3 localization is not only altered due to cell–cell contact destabilization, but depends directly on the presence of Scribble. To address the question of whether the PDZL motif is important for DLC3 localization, we generated MCF7 cells stably expressing full-length GFP–DLC3 and the ΔPDZL variant, and analyzed the cells by immunostaining. Interestingly, PDZL motif deletion impaired the clustering of both WT and GAP-inactive DLC3 at cell–cell contacts (Fig. 3D; Fig. S2D). Quantification of the junctional GFP–DLC3 signal further confirmed the loss of DLC3 accumulation at cell adhesions upon PDZL deletion (Fig. 3E). Taken together, these results provide evidence that the PDZL motif controls the localization of DLC3 at cell–cell contacts.

DLC3 regulates Rho-ROCK signaling to maintain cell-cell contacts and Scribble localization

To directly assess whether RhoA activity at cell–cell adhesions depended on DLC3 expression, we employed the GFP–Anillin AHPH location biosensor for active RhoA. This biosensor encodes the C-terminal part of the scaffold protein anillin, which specifically binds GTP-RhoA (Piekny and Glotzer, 2008; Priya et al., 2015). MCF7 cells transiently transfected with non-targeting (spNT) or DLC3-specific (spDLC3) siRNAs were co-transfected with plasmids encoding the WT biosensor and, as a control, a mutant deficient in RhoA binding (GFP–Anillin AHPH DM) (Fig. 4A). Efficient downregulation of DLC3 was verified by quantitative PCR (Fig. 4C). In control cells, the WT biosensor was distributed evenly in the cells, with no obvious signs of locally elevated RhoA activation. However, in DLC3-depleted cells, GFP–Anillin AHPH WT was enriched in many small aggregates all along the destabilized cell–cell contacts, whereas the control construct exhibited uniform cytoplasmic and nuclear localization (Fig. 4A).

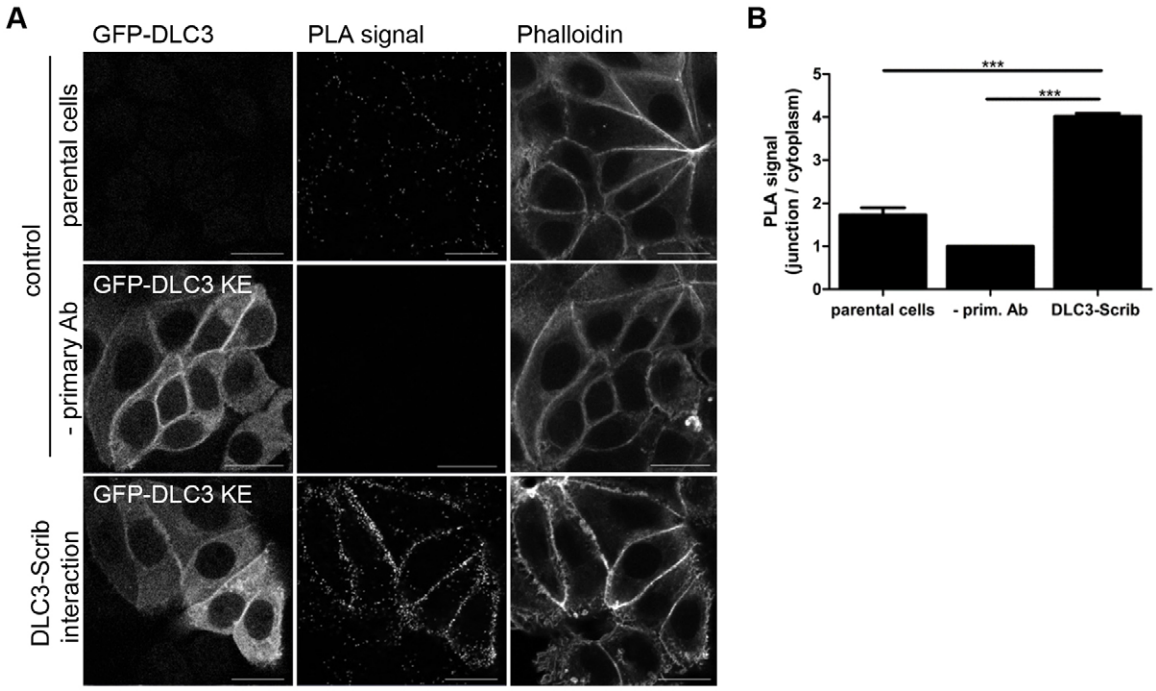

Fig. 2. DLC3 interacts with Scribble *in situ* at cell–cell adhesions. (A) MCF7 cells stably expressing GFP–DLC3 K725E and parental cells as a control were analyzed by *in situ* PLA using anti-GFP and anti-Scribble antibodies. As an additional control, the reaction was performed without primary antibody. Protein–protein interactions are visualized as distinct spots (PLA signal). F-actin was stained with Alexa-Fluor-633-labeled phalloidin. (B) Quantification (mean±s.e.m.) of the junctional to cytoplasmic fluorescence intensity ratio of the PLA signal (n=20 cells; N=3). ***P<0.001 (one-way ANOVA).

Journal of Cell Science (2016) 129, 3583-3596 doi:10.1242/jcs.190074

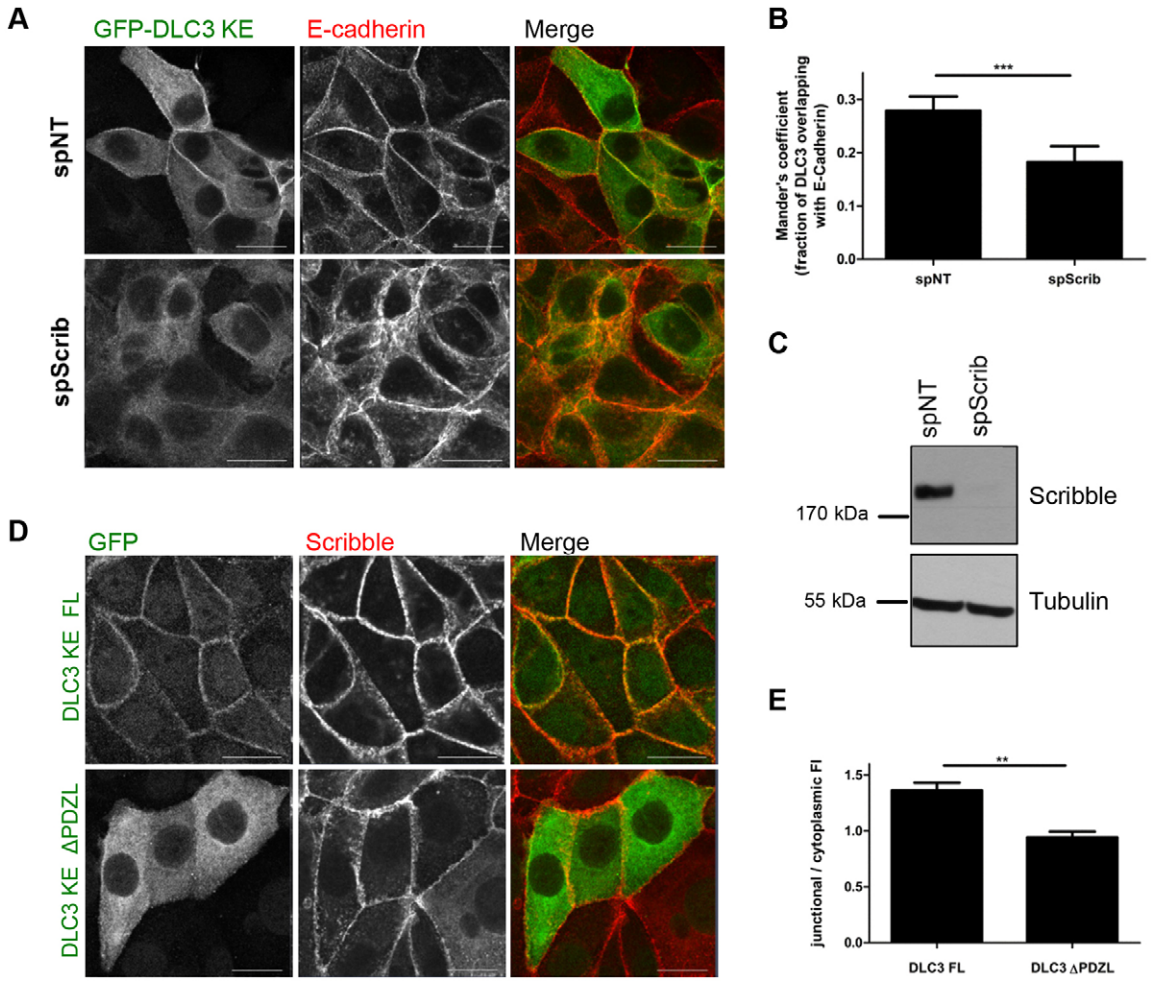

Fig. 3. DLC3 accumulation at cell–cell contacts depends on its PDZ ligand motif and on Scribble. (A) MCF7 cells stably expressing GFP–DLC3 K725E were transfected with non-targeting (spNT) and Scribble-specific (spScrib) siRNAs, respectively. At 72 h post transfection, cells were fixed and stained with GFP- and E-cadherin-specific antibodies. (B) Quantification (mean±s.e.m.) of the fraction of DLC3 overlapping with E-cadherin by Mander's colocalization coefficient (n=12; N=3). (C) Whole-cell lysates of MCF7 cells were analyzed by immunoblotting with anti-Scribble and anti-tubulin antibodies. (D) Stable MCF7 cells expressing GFP–DLC3 K725E full-length (FL) or ΔPDZL were stained with anti-GFP and anti-Scribble antibodies. The images shown are maximum intensity projections of several confocal sections. (E) Quantification (mean±s.e.m.) of the junctional to cytoplasmic fluorescence intensity (FI) ratio of GFP–DLC3 FL and ΔPDZL (n=20 cells; N=3). **P<0.01; ***P<0.001 (paired t-test). Scale bars: 20 µm.

Quantification of the junctional biosensor signal revealed a significant increase in the DLC3-knockdown cells in comparison to the control samples, supporting a role for DLC3 as a RhoGAP at cell adhesions (Fig. 4B). This is in line with the elevated junctional staining of the ROCK substrate phospho-myosin light chain (pMLC) upon DLC3 depletion (Fig. S3A).

To investigate the impact of DLC3 depletion on Scribble localization, MCF7 cells transfected with non-targeting (spNT) and DLC3-specific (spDLC3) siRNAs were stained for Scribble, E-cadherin and F-actin. The junctional association of Scribble, as seen in the control cells, was abrogated by DLC3 knockdown, which was also characterized by impaired cell–cell adhesions (Fig. 4D,E). Interestingly, treatment of DLC3-depleted cells with ROCK (H1152) or Rho (CT04) inhibitor not only rescued the disruption of cell–cell contacts, but also restored Scribble localization (Fig. 4D,E). These data imply a mutual dependence of DLC3 and Scribble: on the one hand, Scribble localization depends on properly balanced RhoA–ROCK signaling at cell junctions controlled by the RhoGAP function of DLC3, on the other hand, DLC3 targeting to cell–cell contacts relies on the scaffolding function of Scribble.

A targeted GAP domain rescues adherens junctions destabilization upon DLC3 knockdown

The N-terminal LRR domains target the Scribble protein to the basolateral membrane and are important for its role in the establishment and maintenance of cell polarity (Navarro et al., 2005; Zeitler et al., 2004). To interrogate whether the GAP domain of DLC3 is sufficient for local Scribble-mediated regulation of Rho signaling, we artificially recruited the DLC3 GAP domain to cell–cell adhesions by fusing it to the LRR domains of Scribble. MCF7 cells stably expressing the GFP-tagged targeted WT GAP domain were generated and, as controls, cell lines stably expressing the targeted inactive GAP domain and LRR only. Then, gene silencing was performed using a DLC3-specific siRNA (siDLC3#1) that does not target the DLC3 GAP domain. LRR-mediated targeting was successful, as seen by the colocalization of LRR, LRR–GAP WT and LRR–GAP K725E with E-cadherin in the stable control cells (Fig. 5A, left panel). Upon DLC3 depletion, cell–cell adhesions were disrupted in MCF7 cells expressing LRR alone or the inactive targeted GAP domain, which was accompanied by the redistribution of the LRR fusion proteins. Remarkably, LRR-mediated targeting

Journal of Cell Science (2016) 129, 3583-3596 doi:10.1242/jcs.190074

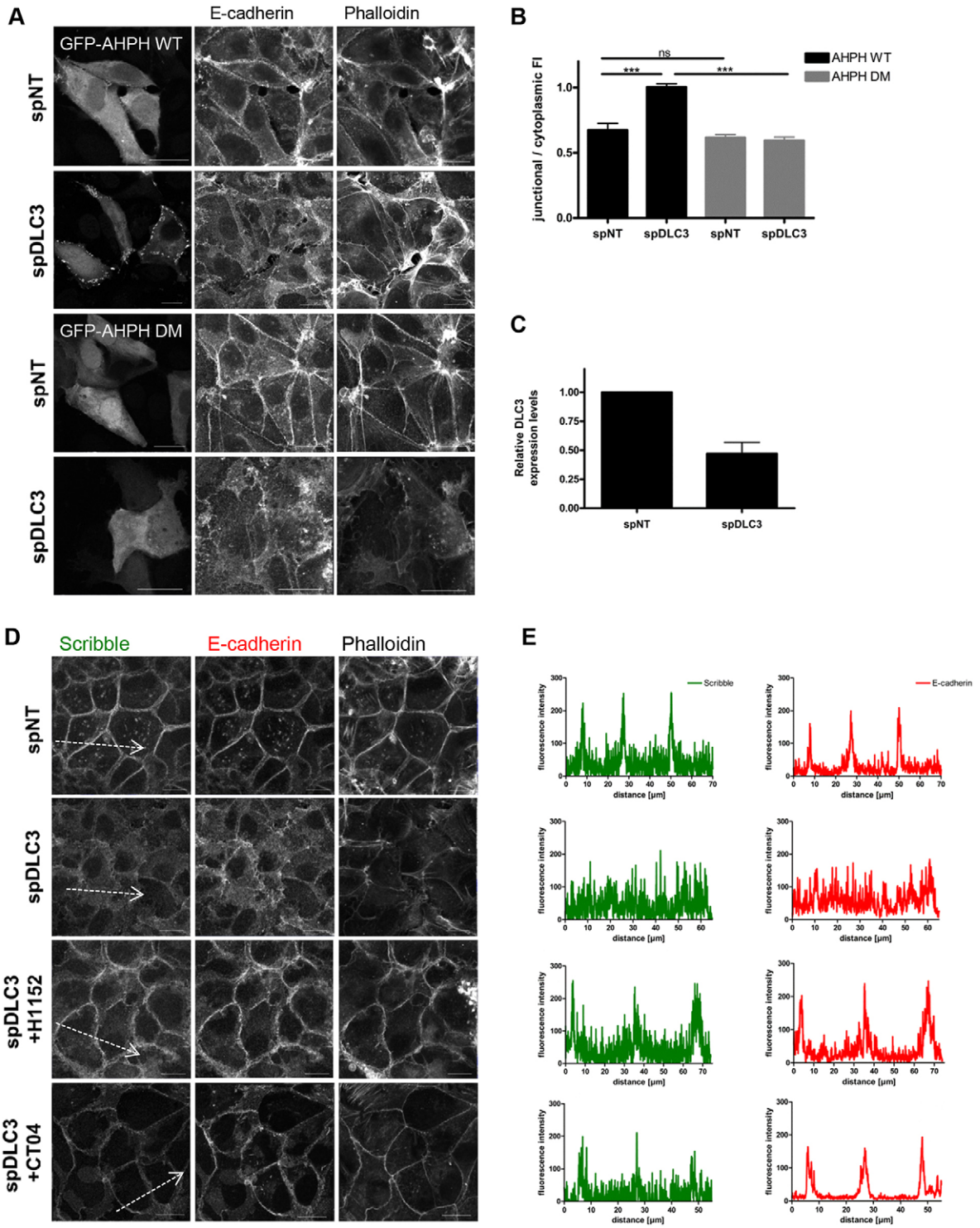

Fig. 4. DLC3 depletion enhances RhoA activity at cell–cell adhesions and impairs Scribble localization in a Rho-ROCK-dependent manner. MCF7 cells were transfected with non-targeting (spNT) or DLC3-specific (spDLC3) siRNAs. (A) After 2 days, cells were transfected with plasmids encoding GFP–Anillin AHPH and A70D/E758K (DM), respectively. The next day, cells were fixed and stained for E-cadherin and F-actin (phalloidin). (B) Quantification (mean±s.e.m.) of the junctional to cytoplasmic fluorescence intensity (FI) ratio of the GFP–AHPH reporter (n=20 cells; N=3). ***P<0.001; ns, not significant (one-way ANOVA). (C) RNA was extracted 72 h later and relative DLC3 expression levels normalized to PPIA as a control gene were determined by quantitative PCR (N=2). (D) After 2 days, cells were treated with ROCK inhibitor overnight (H1152; 10 µM) or on day 3 with Rho inhibitor (CT04; 50 ng/ml) for 5 h where indicated. Cells were fixed and stained for Scribble, E-cadherin and F-actin (phalloidin). The images shown are maximum intensity projections of several confocal sections. (E) The fluorescence intensities of Scribble and E-cadherin along the white arrows in D are depicted. Scale bars: 20 µm.

of the WT DLC3 GAP domain rescued the disorganized E-cadherin staining and preserved the localization of the fusion protein to cell–cell adhesions (Fig. 5A, right panel; Fig. 5B). To quantify the amount of cell junction stability that depended on targeted GAP activity, we next performed cell disaggregation assays in stable MCF7 cells expressing the LRR–GAP fusion proteins (Fig. 5C). In

Journal of Cell Science

Journal of Cell Science (2016) 129, 3583-3596 doi:10.1242/jcs.190074

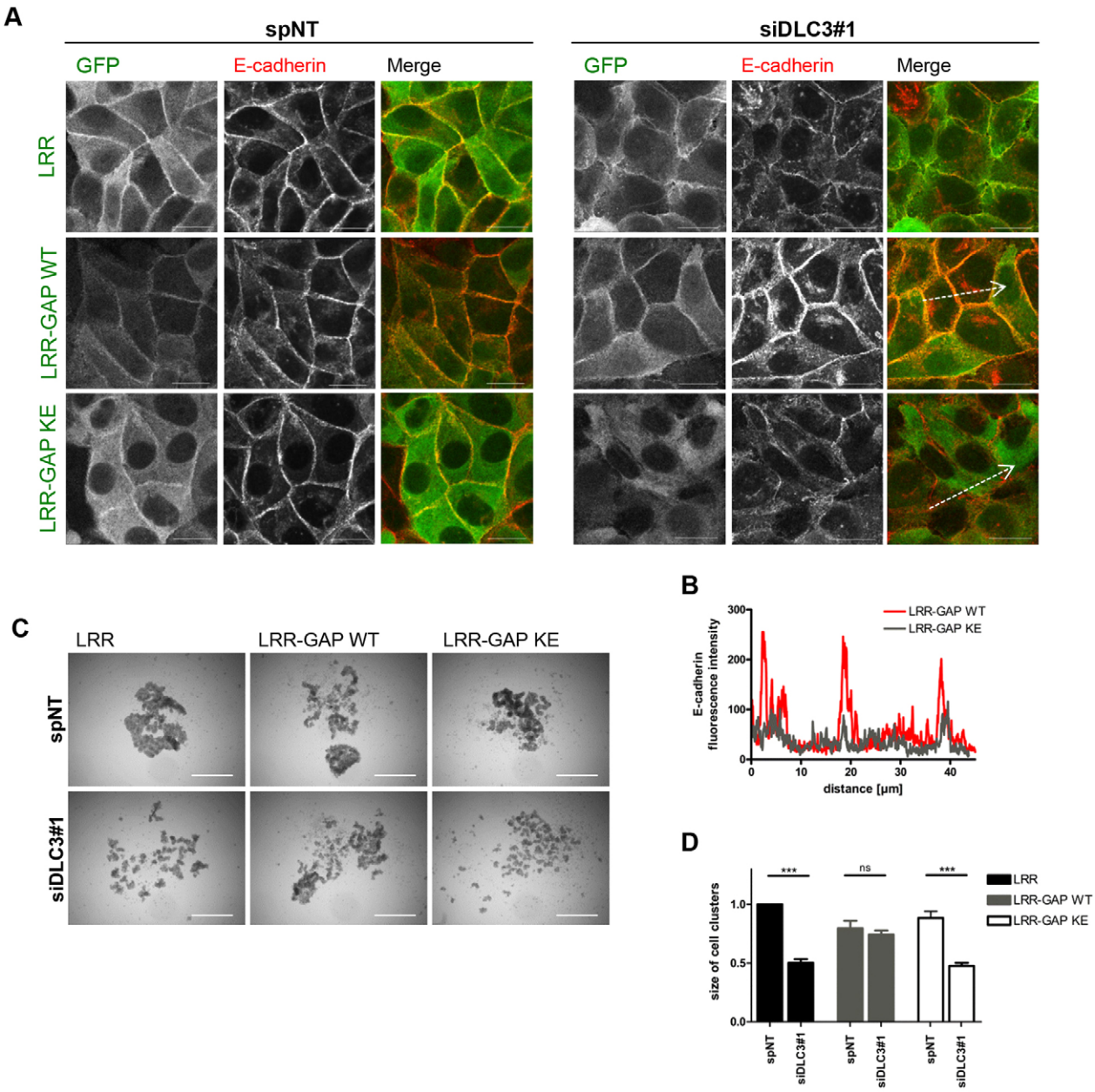

Fig. 5. Targeting of the DLC3 GAP domain to cell–cell contacts by the Scribble LRR domains rescues adherens junction destabilization upon DLC3 knockdown. Stable MCF7 cells expressing GFP–Scribble LRR, LRR–DLC3 GAP WT or K725E, respectively, were transfected with non-targeting (spNT) or DLC3-specific (siDLC3#1) siRNAs. (A) At 72 h post transfection, cells were fixed and stained with GFP- and E-cadherin-specific antibodies. The images shown are maximum intensity projections of several confocal sections. Scale bars: 20 µm. (B) The fluorescence intensities of the E-cadherin signal along the white arrows in A are depicted. (C) At 72 h post transfection, cells were seeded in hanging drops. The next day, cell aggregates were dissociated by pipetting and photographed. Scale bars: 1 mm. (D) Quantification of the cell disaggregation shown in C. The area covered by cell clusters larger than 40,000 µm^2 was determined (mean±s.e.m. of 40 cell clusters derived from two independent experiments). ***P<0.001; ns, not significant (one-way ANOVA).

LRR- and LRR-GAP K725E-expressing control cells, DLC3 knockdown enhanced cell disaggregation by 50% as determined by quantification of cell cluster sizes (Fig. 5D). However, in accordance with our immunofluorescence data, LRR-mediated targeting of a functional DLC3 GAP domain completely rescued the cell disaggregation induced by DLC3 depletion (Fig. 5D). Moreover, increased cell disaggregation in DLC3-depleted cells was partially restored by pharmacological ROCK inhibition (Fig. S3B,C). Taken together, these findings prove that DLC3 functions as a junction-associated regulator of RhoA–ROCK signaling (Holeiter et al., 2012) and junctional positioning of the active GAP protein by Scribble is crucial for its role in maintaining adherens junction integrity.

The PDZL motif mediates basolateral DLC3 localization in polarized Caco-2 cysts

To analyze whether the PDZL-mediated interaction of DLC3 and Scribble is also relevant in other cellular systems, we generated Caco-2 colorectal carcinoma cells inducibly expressing the different DLC3 variants. We then switched on the expression of GAP-inactive, full-length DLC3 and the DLC3 PDZL deletion mutant proteins by treatment with doxycycline in established 2D

Journal of Cell Science (2016) 129, 3583-3596 doi:10.1242/jcs.190074

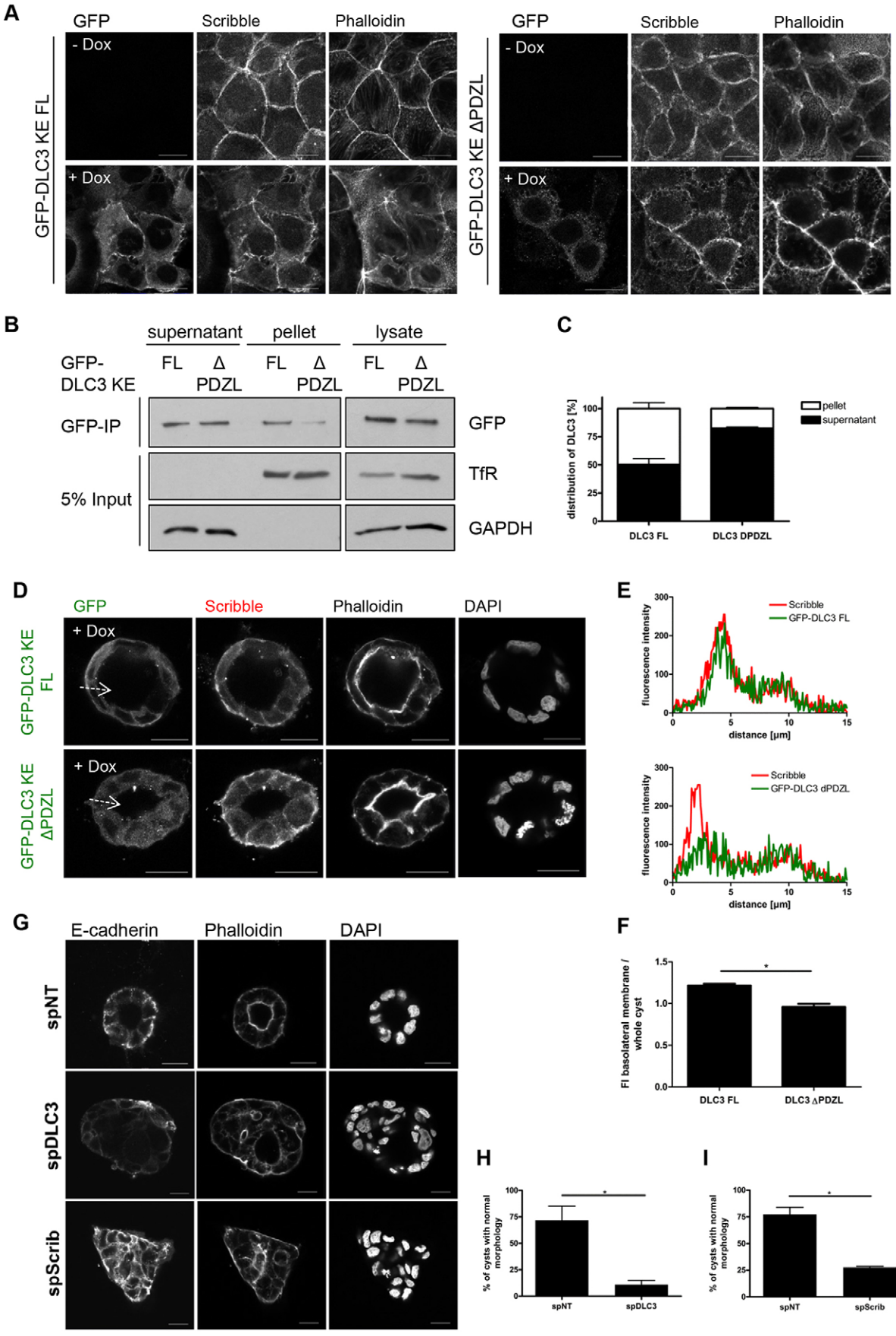

Fig. 6. See next page for legend.

Journal of Cell Science (2016) 129, 3583-3596 doi:10.1242/jcs.190074

Fig. 6. The PDZ ligand motif determines DLC3 localization in polarized Caco-2 cysts and DLC3 or Scribble knockdown cause aberrant cyst morphogenesis. (A) Caco-2tet GFP–DLC3 K725E full-length (FL) and ΔPDZL cells were grown on glass coverslips for 7 days. Where indicated, DLC3 expression was induced by addition of 2 µg/ml dox for 10 h. Cells were fixed and stained for GFP, Scribble and F-actin (phalloidin). The images shown are confocal sections of representative cells. (B) Caco-2tet GFP–DLC3 K725E FL and ΔPDZL (Δ) cells were seeded and, the next day, DLC3 expression was induced with doxycycline for 10 h. Cellular fractions were generated and GFP–DLC3 was enriched by anti-GFP immunoprecipitation. Fractions and immunopurified proteins were analyzed by immunoblotting with anti-GFP, anti-transferrin receptor (TfR) and anti-GAPDH antibodies. (C) Quantification (mean±s.e.m.) of the distribution of DLC3 FL and ΔPDZL in the supernatant and pellet fractions (N=2). (D) Caco-2tet GFP–DLC3 K725E FL and ΔPDZL cells were grown in 3D matrigel culture. At 3 days post seeding, cholera toxin was added to induce lumen formation. The next day, DLC3 expression was induced by doxycycline addition for 10 h. Cultures were fixed and stained as described in A. Nuclei were counterstained with DAPI. Shown are maximum intensity projections of confocal sections of the midplane of representative cysts. (E) The fluorescence intensities of GFP–DLC3 and Scribble along the white arrows in D are depicted. (F) Quantification (mean±s.e.m.) of the fluorescence intensity (FI) ratio of the basolateral signal to that of the whole cyst of GFP–DLC3 K725E FL and ΔPDZL, respectively (n≥12; N=3). (G) Caco-2 cells were transfected with non-targeting (spNT), DLC3-specific (spDLC3) or Scribble-specific (spScrib) siRNAs, respectively. The next day, cells were seeded in 3D cultures containing 10 ng/ml EGF. After 3 days, lumen formation was induced by cholera toxin. The next day, cultures were fixed and stained with an anti-E-cadherin antibody and phalloidin (F-actin). Nuclei were counterstained with DAPI. Shown are confocal sections of the midplane of representative cysts. (H,I) The percentage (mean±s.e.m.) of Caco-2 cysts with normal morphology was determined (n=100; N=3). *P<0.05 (paired t-test). Scale bars: 20 µm.

monolayers (Fig. 6A). Full-length DLC3 accumulated at cell junctions where it colocalized with endogenous Scribble (Fig. 6A) and interaction of full-length GFP–DLC3 with endogenous Scribble was also confirmed biochemically (Fig. S4A). In full accordance with the results obtained in stable MCF7 cells, as opposed to full-length DLC3, DLC3 ΔPDZL was distributed uniformly in the cells (Fig. 6A). To quantify PDZL-motif-dependent subcellular distribution of DLC3, we performed fractionation of cells treated with doxycycline for 10 h only to avoid saturation with excessive protein. Prior to immunoblotting, the GFP–DLC3 proteins were enriched by immunoprecipitation from the supernatant fraction containing soluble cytosolic proteins and the pellet fraction containing detergent-soluble proteins. Compared to the full-length protein, the amount of DLC3 ΔPDZL in the detergent-soluble fraction was clearly reduced (Fig. 6B,C), supporting the idea that the PDZL motif is required for membrane recruitment of DLC3.

We then analyzed DLC3 localization and function in 3D matrigel cultures of Caco-2 cells, which form polarized cysts consisting of a single epithelial cell layer with apical-basolateral polarity surrounding a hollow lumen. Expression of DLC3 WT in fully established cysts led to the collapse of lumens, whereas Caco-2 cysts expressing GAP-inactive DLC3 K725E retained their polarized morphology associated with basolateral Scribble and apical F-actin accumulation (Fig. S4B; Fig. 6D). Consistent with the results in 2D monolayers, full-length DLC3 colocalized with Scribble at the basolateral membrane, which was significantly reduced by PDZL deletion (Fig. 6D-F). Taken together, our findings show that the PDZL motif is essential for the basolateral membrane localization of DLC3 in polarized Caco-2 cells and highlight the importance of properly balanced DLC3 GAP activity for the maintenance of the polarized morphology. Unfortunately, based on the quantification of the number of cysts with a normal polarized morphology, we could not demonstrate any altered biological function for GAP-competent DLC3 ΔPDZL (Fig. S4C), which is most likely due to the saturation of cells with overexpressed protein. To assess such functional differences, DLC3 expression should be driven by a weaker promoter.

DLC3 and Scribble are required for polarized lumen formation of Caco-2 cysts

Finally, we knocked down DLC3 and Scribble before seeding of cells into 3D matrigel cultures containing EGF. Previous studies have shown that EGF stimulates proliferation of Caco-2 cells, leading to a larger size of cysts, but it does not interfere with polarized cyst development (Möller et al., 2014). After 3 days, lumen formation was induced with cholera toxin and, the next day, the cysts were fixed and stained for E-cadherin and F-actin as basolateral and apical markers, respectively (Fig. 6G). Efficient downregulation of DLC3 and Scribble was confirmed by quantitative PCR and immunoblotting, respectively (Fig. S4G,H). We found that, upon DLC3 and Scribble knockdown, Caco-2 cells failed to form cysts with a single lumen and distinct apical F-actin staining, and E-cadherin distribution was no longer restricted to basolateral membranes. DLC3 and Scribble depletion resulted in similar phenotypes characterized by the formation of flat and spread multicellular structures with multiple or no lumens (Fig. 6G). Quantification revealed that more than 70% of the Caco-2 control cysts developed normally, as assessed by their round morphology, well-defined apical F-actin staining and the presence of a single apical lumen. By contrast, DLC3 and Scribble knockdown caused a significant reduction of cysts with normal morphology (11% and 28%, respectively; Fig. 6H,I), which was confirmed by independent siRNAs targeting DLC3 and Scribble (Fig. S4D–H). Taken together, these data provide evidence that DLC3 and Scribble are both required for polarized epithelial morphogenesis and lumen formation of Caco-2 cells.

DISCUSSION

Here, we identify the basolateral polarity protein Scribble as the first isoform-specific DLC3-binding partner, and show that it recruits the RhoGAP DLC3 to cell–cell contacts. This interaction is mediated by the PDZ domains of Scribble and a unique C-terminal PDZL motif in DLC3. Using a location biosensor for active RhoA and a LRR-targeted GAP domain, we show that DLC3 is required for local RhoA regulation at cell–cell adhesions and uncover a mutual dependence of DLC3 and Scribble: on the one hand, Scribble acts as a scaffold to recruit DLC3, ensuring locally restricted Rho activity at cell junctions and basolateral membranes; on the other hand, DLC3 as a negative regulator of Rho–ROCK signaling is required for adherens junction maintenance and, consequently, Scribble localization at cell–cell contacts.

Scribble targets the RacGEF protein β-Pix to the basolateral membrane where it promotes Rac activation (Frank et al., 2012; Zhan et al., 2008). By additionally recruiting the RhoGAP protein DLC3 to suppress RhoA activation as revealed by our work, Scribble contributes in a dual manner to the establishment of antagonizing Rho and Rac activity gradients in epithelial cells. Apart from Scribble, it is possible that further PDZ domain proteins might be involved in the control of DLC3 localization and function. Considering that our proteomic analysis detected several components of the syntrophin–utrophin–dystrobrevin complex, which constitutes a scaffold for mechanical stabilization during contraction in muscle cells, DLC3 might possess yet unknown functions in such cells (Albrecht and Froehner, 2002). Recently,

Journal of Cell Science (2016) 129, 3583-3596 doi:10.1242/jcs.190074

β2-syntrophin was also shown to be crucial for junction assembly and apical-basal polarity in epithelial cells (Mack et al., 2012), thus syntrophins, as alternative scaffolds, might support Scribble in the junctional recruitment of DLC3. Biochemical experiments showed that the DLC3–Scribble interaction is mediated mainly by the Scribble PDZ3 domain, which also interacts with the planar cell polarity protein Vangl (Courbard et al., 2009). In striking contrast to its role as a tumor suppressor, in breast cancer cells Scribble association with a NOS1AP–Vangl complex at lamellipodia was correlated with enhanced cell migration and tumor progression (Anastas et al., 2012). Considering that DLC3 has a potential tumor-suppressive function, it is tempting to speculate that DLC3 can compete with Vangl proteins for Scribble binding, thereby modulating the tumor-suppressive versus oncogenic functions of Scribble. Alternatively, loss of the membrane-bound localization of Scribble, which is associated with a gain of tumor-promoting properties (Elsum and Humbert, 2013), might result in cytoplasmic DLC3 sequestration reminiscent of a mechanism recently described for PTEN (Feigin et al., 2014), thereby comprising the function of DLC3 in cell adhesion and increasing cell motility.

Our findings reveal that the C-terminal PDZ ligand motif in DLC3 is required for the recruitment of the protein to cell–cell contacts and, in polarized cells, to basolateral membranes. In addition, other domains contribute to DLC3 subcellular localization and membrane association. For example, we have previously shown that the SAM domain targets DLC3 to Golgi membranes (Braun et al., 2015), whereas a polybasic region conserved in all DLC isoforms mediates the binding to phosphatidylinositol-4,5-bisphosphate-enriched membranes (Erlmann et al., 2009). Considering the importance of the PDZL motif for proper DLC3 localization, it is intriguing that in different types of cancer mutations in the DLC3 coding sequence are reported (http://www.cbioportal.org), some of which produce a premature stop codon (DLC3 E686*; DLC3 A874S fs*16), yielding proteins that leave the GAP domain intact but lack the PDZL motif. Based on our data, these DLC3 mutant proteins are expected to be mislocalized from cell adhesions and thus functionally inactive with respect to RhoA regulation at these sites. Junctional recruitment of DLC3 by its PDZL motif is an isoform-specific regulatory mechanism because the DLC family members DLC1 and DLC2 lack this motif and consequently they do not interact with Scribble. DLC1 was also reported to associate with cell–cell contacts by binding α-catenin in a GAP-dependent manner (Tripathi et al., 2012), whereas DLC2 was shown to control junction integrity by affecting microtubule growth and spindle positioning through Cdc42–mDia signaling (Vitiello et al., 2014). Thus, although the DLC proteins were initially believed to possess largely overlapping cellular functions, these observations support the idea that isoform-specific functions are conferred by their different subcellular localizations associated with the regulation of spatially distinct Rho GTPase pools.

Depletion of Scribble has been shown to impair E-cadherin function resulting in adherens junction destabilization, enhanced cell disaggregation and migration (Qin et al., 2005). The DLC3-knockdown phenotype exhibits very similar characteristics, indicating that the physical interaction of DLC3 and Scribble translates into a functional biological interaction. However, in the MCF10A model of breast epithelial morphogenesis, loss of DLC3 or Scribble has no obvious effect on polarized acini formation (Dow et al., 2006; Holeiter et al., 2012). This contrasts with our results in Caco-2 cells, in which the absence of DLC3 or Scribble resulted in prominent polarity defects associated with impaired lumenogenesis. However, it is important to note that only in the presence of EGF did we observe aberrant polarized morphogenesis of DLC3 and Scribble-knockdown cells. This is in line with the observation that specific oncogene activation or cytokine exposure cooperates with the loss of Scribble to disrupt cell polarity and cause an invasive phenotype in MCF10A cells (Chatterjee et al., 2012). Considering that DLC3 and Scribble are both involved in coordinating endocytic membrane trafficking, and EGF increases E-cadherin turnover (Bryant et al., 2007), the aberrant morphogenesis of DLC3 and Scribble depleted cysts might also be linked to altered vesicular transport. In particular, DLC3 is implicated in recycling processes driven by Rab8 (Braun et al., 2015), an important regulator of lumenogenesis (Bryant et al., 2010), whereas Scribble is involved in the control of E-cadherin internalization and retromer-dependent retrograde transport (de Vreede et al., 2014; Lohia et al., 2012). Thus, in addition to their local function at adherens junctions, the coordination of membrane trafficking by Scribble and DLC3 might be required for the correct distribution of proteins in polarized epithelial cells. In future studies, it will be interesting to explore the dynamics of the DLC3–Scribble interaction and whether complex formation is restricted to adherens junctions. Moreover, the molecular mechanisms, such as posttranslational modifications that regulate DLC3 interaction with Scribble and other protein binding partners remain to be explored. For example, the isolation of several proteins involved in proteasomal degradation, including the ubiquitin ligases HUWE-1 and CHIP (Table S1), provides a hint that DLC3 might be regulated by ubiquitylation. Elucidating in more depth the physiological functions of DLC3 and its molecular regulation will help to better understand how its functional inactivation might contribute to tumor progression.

MATERIALS AND METHODS

Antibodies and reagents

Antibodies used were: monoclonal mouse anti-E-cadherin (immunofluorescence 1:250; cat. no. 610182, BD Transduction Laboratories, Heidelberg, Germany); monoclonal rabbit anti-E-cadherin (immunofluorescence 1:200) and polyclonal rabbit anti-phospho-myosin light chain 2 (pMLC; Ser19; immunofluorescence 1:50) (cat. nos. 3195 and 3671, respectively, Cell Signaling, Danvers, MA); polyclonal goat anti-GST (western blotting 1:5000; cat. no. GE-27-4577-01, GE Healthcare, Piscataway, NJ); monoclonal mouse anti-TfR (western blotting 1:1000; cat. no. 13-6800, Invitrogen, Carlsbad, CA); monoclonal mouse anti-GFP (immunofluorescence 1:250; western blotting 1:2000; cat. no. 11 814 460 001, Roche Biosciences, Basel, Switzerland); monoclonal mouse anti-Cbl (A-9; as a control IgG for co-immunoprecipitation), anti-DLC3 (E-2; western blotting 1:500), polyclonal goat anti-Scribble (C-20; western blotting 1:250) and polyclonal rabbit anti-Scribble (H-300; immunofluorescence 1:100) (cat. nos c-1651, sc-166725, sc-11049 and sc-28737, respectively, Santa Cruz Biotechnology, Dallas, TX); monoclonal mouse anti-α-tubulin (western blotting 1:2000, anti-Flag M2 (western blotting 1:2000), rabbit anti-GAPDH (1:15,000) (cat. nos T5168, F3165 and G9545, respectively, Sigma-Aldrich, St Louis, MO); HRP-labeled secondary anti-mouse (western blotting 1:1000), anti-rabbit (western blotting 1:1000) and anti-goat (western blotting 1:10,000) IgG (GE Healthcare); Alexa Fluor®-labeled secondary IgG (immunofluorescence 1:500) (Invitrogen). Alexa-Fluor®-labeled phalloidin was from Invitrogen, DAPI from Sigma-Aldrich, EGF from R&D Systems Inc. (Minneapolis, MN), H1152 from Calbiochem (Darmstadt, Germany) and Rho Inhibitor I (CT04) from Cytoskeleton (Denver, CO).

DNA constructs

pEGFP-C1-DLC3α WT/K725E, pEGFP-C1-DLC1, pEGFP-C1-DLC2α, pCR.V62-Met-Flag-DLC3α WT/K725E vectors were described previously (Braun et al., 2015; Erlmann et al., 2009; Holeiter et al., 2012). pEGFP-C1-Anillin AHPH WT and A70D/E758K (DM) were provided by Alpha Yap

Journal of Cell Science (2016) 129, 3583-3596 doi:10.1242/jcs.190074

(University of Queensland, Australia) (Piekny and Glotzer, 2008; Priya et al., 2015). Expression vectors encoding GFP-tagged human (h)Scribble, pDEST15-GST-PDZ1 hScribble, pDEST15-GST-PDZ2 hScribble, pDEST15-GST-PDZ3 hScribble and pDEST15-GST-PDZ4 hScribble were provided by Jean-Paul Borg (Centre de Recherche en Cancérologie de Marseille, France). pCR.V62-Met-Flag DLC3 WT and K725E ΔPDZL vectors were generated by PCR amplification using pCR.V62-Met-Flag-DLC3α WT and K725E as a template, respectively, and the following forward and reverse primers: 5′-CCGGAATTCCCTCTGCTGGACGTT-TTCTG-3′ and 5′-CCGGAATTCTCAGCCCGCTGCCTGCAGGG-3′. PCR products were cloned into the pCR.V62-Met-Flag vector by EcoRI restriction. pEGFP-C1- DLC3 WT and K725E ΔPDZL were generated by PCR amplification using pEGFP-C1-DLC3 WT and K725E as a template, respectively, and the following forward and reverse primers: 5′-CCGGAATTCTCCTCTGCTGGACGTTTTCTG-3′ and 5′-CCGGAA-TTCTCAGCCCGCTGCCTGCAGGG-3′. PCR products were cloned into pEGFP-C1 by EcoRI restriction. pEGFP-C1-Scribble LRR was obtained by PCR amplification of the Scribble LRR (amino acids 1–420) using GFP–hScribble as a template and the following forward and reverse primers: 5′-CCGGAATTCCATGCTCAAGTGCATCCCGCTG-3′ and 5′-CCGGT-CGACGGGCTGCTGGGGCAGCAA-3′. The PCR product was cloned into pEGFP-C1 by EcoRI/SalI restriction. pEGFP-C1-Scribble LRR-DLC3 GAP WT/K725E were generated by subcloning of the respective GAP domains from pEGFP-C1-DLC3-SAM-GAP WT/K725E (Braun et al., 2015) into pEGFP-C1-Scribble LRR lacking a stop codon by SalI restriction. pWHE636-GFP-DLC3 full-length and ΔPDZL (GAP WT/K725E) were generated by PCR amplification using pEGFP-C1-DLC3 full-length or ΔPDZL (GAP WT/K725E) as templates, forward primer 5′-CCGGCGGCCGCATGGTGAGCAAGGGCGAGGAC-3′ and reverse primers 5′-CCGGCGGCCGCTCACAGCTTTGTCTCAGGGCCC-3′ for the full-length and 5′-CCGGCGGCCGCTCAGCCCGCTGCCTGCAGG-G-3′ for the ΔPDZL constructs, respectively. PCR products were cloned into pWHE636 (provided by Tilman Brummer, University of Freiburg, Germany) by NotI restriction. pGEX-6P-3-GST-Scribble PDZ1-4 was obtained by PCR amplification of Scribble PDZ1–PDZ4 (amino acids 728–1194) using GFP–hScribble as a template and the following forward and reverse primers: 5′-CCGGAATTCCACCCTCACCATCCTGCGGC-3′ and 5′-CCGGTCGACTCAGGCCTCGAAGCCGTCACAG-3′. The PCR product was cloned into pGEX-6P-3 by EcoRI/SalI restriction. Amplified cDNAs were verified by sequencing. Oligonucleotides were from Eurofins MWG Operon (Ebersberg, Germany).

NanoLC-MS/MS analysis and mass spectrometry data processing

Flag-tagged proteins were immunoprecipitated from cell lysates (see NEB buffer, containing 1% Triton X-100 instead of NP-40) with Flag M2 agarose (Sigma-Aldrich). Beads were washed with 1% TEB and PBS followed by elution with 0.1 M glycine (pH 2.5) and neutralization with a 1/10 volume of 1 M Tris-HCl (pH 8.0). Protein expression and immunopurification were verified by parallel immunoblotting. Eluates were loaded on a NuPAGE Bis-Tris 4–12% gradient gel (Invitrogen) for a short gel run and proteins were in-gel digested with trypsin (Borchert et al., 2010). Peptide mixtures were separated on the EasyLC nano-HPLC (Thermo Scientific) coupled to an LTQ Orbitrap Elite (Thermo Scientific). Binding and chromatographic separation of peptides was performed on a 15-cm fused silica emitter of 75 µm inner diameter (Proxeon Biosystems), in-house packed with reversed-phase ReproSil-Pur C18-AQ 3-µm resin (Dr Maisch GmbH). Peptide mixtures were injected in HPLC solvent A (0.5% acetic acid) at a flow rate of 500 nl/min and subsequently eluted with an 87-min segmented gradient of 10–50% HPLC solvent B (80% acetonitrile in 0.5% acetic acid) at a flow rate of 200 nl/min. The mass spectrometer was operated in the data-dependent mode to automatically switch between MS and MS/MS acquisition. Precursor ions were acquired in the mass range from *m*/*z* 300–2000 in the Orbitrap mass analyzer at a resolution of 120,000. The accumulation target value was set to 10^6 charges. The 20 most intense ions were sequentially isolated and fragmented in the linear ion trap using collision-induced dissociation (CID) at the ion accumulation target value of 5000 and default CID settings. Ions already selected for MS/MS were dynamically excluded for 60 s. Acquired MS spectra were processed with MaxQuant software package version 1.5.2.8 (Cox and Mann, 2008) with integrated Andromeda search engine (Cox et al., 2011). Database searching was performed against a target decoy *Homo sapiens* database obtained from Uniprot, containing 91,675 protein entries and against databases containing sequences of different Flag-tagged DLC3 variants and 245 commonly observed contaminants. Endoprotease trypsin was defined as the protease with a maximum missed cleavage of two. Oxidation of methionine and N-terminal acetylation were specified as variable modifications, whereas carbamidomethylation on cysteines was defined as a fixed modification. Initial maximum allowed mass tolerance was set to 4.5 ppm (for the survey scan) and 0.5 Da for CID fragment ions. A false discovery rate of 1% was applied at the peptide and protein level. The iBAQ method as implemented in MaxQuant was used for intensity-based absolute quantification (Schwanhausser et al., 2011). Bioinformatic downstream annotation (GOCC and Pfam) analysis was performed using the Perseus Software package version 1.5.0.15.

Cell culture, transfection and generation of stable cell lines

HEK293T (ATCC), HeLa (ATCC), MCF7 (provided by the Institute of Clinical Pharmacology, Stuttgart, Germany) and Caco-2 (Interlab Cell Line Collection, Genova, Italy) cells were cultured in RPMI 1640 (Invitrogen) supplemented with 10% fetal calf serum (FCS; PAA Laboratories, Cölbe, Germany). Caco-2 cells were reauthenticated by SNP analysis in 2016 (Multiplexion, Immenstadt, Germany). All other cell lines were authenticated by morphology and growth characteristics, tested for mycoplasma and cultured for less than 4 months after thawing. In HEK293T cells, plasmid transfections were performed with Turbofect® (Thermo Scientific, Rockford, IL) and in MCF7 cells with Lipofectamine® LTX (Invitrogen). MCF7 cells stably expressing GFP–DLC3 WT or K725E were as described previously (Holeiter et al., 2012). Stable MCF7 cells expressing GFP–DLC3 WT or K725E ΔPDZL and GFP–Scribble LRR and LRR–GAP WT or K725E were generated by transfection of the respective expression vectors followed by 1 mg/ml G418 selection (Calbiochem) and FACS sorting of GFP-positive cells. Caco-2tet cells, stably expressing the doxycycline-inducible system components rtTA and rtTS were as described previously (Röring et al., 2012). Caco-2tet GFP–DLC3 WT or K725E cells and Caco-2tet GFP–DLC3 WT ΔPDZL or K725E ΔPDZL cells were generated by nucleofection (program B024, Kit T, Lonza) of respective pWHE-636-GFP-DLC3 vectors followed by selection with 5 µg/ml blasticidin and 5 µg/ml puromycin. For 3D cultures, Caco-2 cells were seeded on a matrix of growth factor reduced matrigel (BD) and PureCol®-S collagen (Advanced Biomatrix, San Diego, CA) (1:1) and overlaid with growth medium containing 2% matrigel. For knockdown cells, 10 ng/ml EGF (R&D) was added to the medium. Lumen formation was induced by 100 ng/ml cholera toxin (Sigma-Aldrich). Transgene expression in Caco-2tet cells was induced with 2 µg/ml doxycycline (dox; Merck, Darmstadt, Germany).

RNA interference

MCF7 cells were transfected with siRNAs using Lipofectamine® RNAiMAX (Invitrogen) and Caco-2 cells using DharmaFECT1 (Dharmacon, Lafayette, CO). ON-TARGETplus® non-targeting control SMARTpool siRNA (D-001810-10, Dharmacon) was used as a negative control. The following DLC3- and Scribble-specific siRNAs were used: siGENOME SMARTpool human STARD8 (spDLC3) (M-010254, Dharmacon), Silencer®Select human STARD8 (siDLC3#1) (s18825, Invitrogen), Silencer®Select human STARD8 (siDLC3#2) (s18826, Invitrogen), ON-TARGETplus® SMARTpool human Scrib (spScrib) (L-010500-00, Dharmacon), Silencer®Select human Scrib (siScrib#1) (s23970, Invitrogen) and Silencer®Select human Scrib (siScrib#2) (s23971, Invitrogen).

Cell lysis, immunoprecipitation and western blotting

Cells were lysed in RIPA buffer (NEB buffer with 1% NP-40 and additionally containing 0.25% sodium deoxycholate and 0.1% SDS) or for immunoprecipitation in 0.5% NEB buffer [50 mM Tris-HCl pH 7.5, 150 mM NaCl, 0.5% NP-40, 1 mM EDTA, 1 mM sodium orthovanadate,

10 mM sodium fluoride, 0.5 mM PMSF and 20 mM β-glycerophosphate plus Complete protease inhibitors (Roche)]. Lysates were clarified by centrifugation for 10 min at 16,000 ***g*** and 4°C. For immunoprecipitation, equal amounts of protein were diluted with extraction buffer to a final concentration of 0.25% NP-40 and incubated with specific antibodies for 3 h at 4°C. Immune complexes were collected using protein G agarose (KPL) and washed three times with 0.25% NEB. Proteins were separated by SDS-PAGE and transferred to polyvinylidene difluoride membranes (Roth, Karsruhe, Germany). Alternatively, lysates were loaded on 4–12% NuPAGE® Novex Bis-Tris gels (Invitrogen) and transferred to nitrocellulose membranes (iBlot®Gel Transfer Stacks; Invitrogen). Membranes were blocked with 0.5% blocking reagent (Roche) in PBS containing 0.05% Tween 20 and incubated with primary antibodies, followed by HRP-conjugated secondary antibodies. Proteins were visualized by ECL detection (Pierce, Rockford, IL) or, alternatively, IRDye 800 goat anti-GST antibody (antibody against GST, cat. no. 600-132-200, 1:15,000) or IRDye 800 CW goat anti-mouse-IgG (1:15,000), respectively (Licor Biotechnology, Bad-Homburg, Germany). For fractionations, cells were lysed in 50 mM Hepes, pH 7.4, 100 mM NaCl, 5 mM $MgCl_2$, 0.5 mM EDTA, 1 mM DTT, 1 mM sodium orthovanadate, 0.5 mM PMSF plus Complete protease inhibitors. After three freeze–thaw cycles in liquid nitrogen, samples were cleared by centrifugation (20 min, 16,000 ***g***) and the supernatant collected. The pellet was solubilized in 1% NEB buffer, followed by centrifugation (10 min, 16,000 ***g***). Equal amounts of the fractions were diluted in 0.5% NEB buffer (1:1) and enriched by anti-GFP immunoprecipitation. Quantification of immunoblots was performed with ImageJ (NIMH, Bethesda, MD).

Bacterial expression of GST proteins, far western blotting and pulldowns

E.coli were transformed with pDEST15-GST-PDZ1/2/3/4 hScribble, pGEX-6P-3-GST-Scribble PDZ1-4 and empty vector, respectively, and expression was induced with 0.5 mM IPTG for 3 h at 30°C. Bacteria were pelleted and resuspended in PBS containing Complete protease inhibitors. The suspension was sonicated 3× for 10 s on ice, incubated for 15 min and Triton X-100 was added (1% final concentration) before centrifugation for 10 min at 10,000 ***g***. GST-tagged protein was purified with glutathione resin (GE Healthcare) and analyzed by SDS-PAGE and Coomassie staining. For far western blotting, GST–Scribble PDZ1–PDZ4 or GST alone was eluted using 10 mM reduced glutathione in 50 mM Tris-HCl (pH 8.0). Membranes were incubated with 400 nM GST–Scribble PDZ1–PDZ4 or GST in 0.5% blocking reagent (Roche) in PBS containing 0.05% Tween 20 at 4°C overnight. Membranes were washed with PBS containing 0.05% Tween 20, and incubated with primary and HRP-labeled secondary antibodies, followed by ECL detection (Pierce). Pulldowns were performed by incubation of HEK293T cell lysates (in 0.25% NEB buffer) with immobilized GST-tagged proteins. Beads were washed 3× with 0.25% NEB buffer and proteins subjected to SDS-PAGE and immunoblotting.

Immunofluorescence microscopy

Cells grown on coverslips coated with 10 µg/ml collagen R (Serva, Heidelberg, Germany) were fixed with 4% PFA in PBS for 15 min, washed with PBS and incubated in 150 mM glycine in PBS for 15 min. For 3D matrigel cultures, cells were grown on eight-well glass chamber slides coated with matrigel:collagen (1:1) (BD) and fixed with 4% PFA in PBS for 15 min at 37°C. All samples were permeabilized with 0.2% Triton X-100 in PBS for 10 min and blocked with 5% goat serum in PBS containing 0.1% Tween 20 for 30 min. Cells were stained with primary antibodies diluted in blocking buffer, washed with PBS containing 0.1% Tween 20 and incubated with Alexa Fluor® (488, 546 or 633)-labeled secondary antibodies. F-actin and nuclei were counterstained with Alexa-Fluor-labeled phalloidin and DAPI, coverslips were mounted in Fluoromount-G® (Southern Biotech, Birmingham, AL). Samples were analyzed on a confocal laser scanning microscope (LSM710; Zeiss, Oberkochen, Germany) equipped with an oil immersion objective Plan-Apochromat 63×1.40 DIC M27 lens using 488-, 561- and 633-nm excitation. Maximum intensity projections, linear adjustments of brightness and contrast, and acquisition of line scans were performed with ZEN software (Zeiss). For quantification of fluorescence intensities, images were acquired with the same confocal settings and junctional and cytoplasmic signals were measured with ImageJ. The Mander's coefficient was determined using the JACoP plugin (Bolte and Cordelières, 2006). For quantification of polarized Caco-2 cysts, Caco-2 spheroids with a round morphology, a cell-free lumen and distinct F-actin staining of the apical surface were scored as normal, whereas flat cysts with no or multiple lumens were scored as abnormal.

In situ proximity ligation assay

Cells were fixed, permeabilized and stained with primary antibodies (mouse GFP-specific and rabbit Scribble-specific antibody) as described for immunofluorescence analysis. For blocking, the buffer provided by the Duolink system (Sigma-Aldrich) was used. Incubation with PLA probes, ligation and amplification were performed according to the manufacturer's instructions using the detection reagents 'orange'. Cells were stained with Alexa-Fluor-labeled phalloidin and mounted in Dapi-containing Duolink mounting medium. PLA signals were imaged with a confocal LSM710 microscope.

Cell disaggregation assay

Cells were seeded in 25-µl drops (1×10^6 cells/ml) onto the lid of a culture dish and incubated in an inverted manner overnight to allow the formation of cell aggregates. ROCK inhibitor was added 6 h post seeding. The next day, aggregates were pipetted up and down (15× with a 20 µl pipette) and photographed at 2× magnification using an Evos FL cell imaging system [Advanced microscopy group (AMG)]. The area covered by the remaining cell clusters larger than 40,000 μm^2 was quantified using ImageJ.

Quantitative PCR

RNA was isolated with the RNeasy® Plus Mini Kit (Qiagen, Foster City, CA). Q-PCR was performed with QuantiTect Primer Assays® for SYBR® Green-based expression analysis (Qiagen) using a Cfx96 device (Biorad) according to the manufacturer's protocol for one-step RT-PCR. Primers used were 5′-CATGGAGCGCAGGGACC-3′ and 5′-GGGAAGCACTT-CACCTTCCT-3′ for DLC3 (Biomers.net, Ulm, Germany) and Hs_PPIA_4_SG QuantiTect Primer Assay (Qiagen). Changes in the relative expression level were determined using the $2^{-\Delta\Delta Ct}$ method (Biorad CFX manager software 3.1.). PPIA was used as a control gene for normalization.

Statistical analysis

Data are shown as mean±s.e.m.; 'n' refers to the number of analyzed cells, cysts or cell aggregates/experiment and 'N' to the number of independent experiments. Statistical significance was analyzed by *t*-test and one-way ANOVA followed by Tukey's post-test (GraphPad Prism version 4.03; GraphPad Software Inc., La Jolla, CA). *P*-values below 0.05 were considered as significant (*P<0.05; **P<0.01; ***P<0.001; ns, not significant, P>0.05).

Acknowledgements

We thank Angelika Hausser (University of Stuttgart, Germany) for critically reviewing the manuscript and Silke Wahl for technical assistance in MS sample preparation.

Competing interests

The authors declare no competing or financial interests.

Author contributions

J.H. and Y.M. performed experiments and analyzed data; M.F.-M. and B.M. conducted the mass spectrometry analysis; S.S. assisted with protein production; M.A.O. conceived the study and wrote the manuscript together with J.H. and B.M.

Funding

This work was supported by the Deutsche Forschungsgemeinschaft (DFG) through the Heisenberg program [grant number OL239/8-2 to M.A.O.], and the DFG grant [grant number OL239/9-2 to M.A.O.].

Supplementary information

Supplementary information available online at
http://jcs.biologists.org/lookup/doi/10.1242/jcs.190074.supplemental

References

Albertson, R., Chabu, C., Sheehan, A. and Doe, C. Q. (2004). Scribble protein domain mapping reveals a multistep localization mechanism and domains necessary for establishing cortical polarity. *J. Cell Sci.* **117**, 6061-6070.

Albrecht, D. E. and Froehner, S. C. (2002). Syntrophins and dystrobrevins: defining the dystrophin scaffold at synapses. *Neurosignals* **11**, 123-129.

Anastas, J. N., Biechele, T. L., Robitaille, M., Muster, J., Allison, K. H., Angers, S. and Moon, R. T. (2012). A protein complex of SCRIB, NOS1AP and VANGL1 regulates cell polarity and migration, and is associated with breast cancer progression. *Oncogene* **31**, 3696-3708.

Bilder, D. and Perrimon, N. (2000). Localization of apical epithelial determinants by the basolateral PDZ protein Scribble. *Nature* **403**, 676-680.

Bolte, S. and Cordelières, F. P. (2006). A guided tour into subcellular colocalization analysis in light microscopy. *J. Microsc.* **224**, 213-232.

Borchert, N., Dieterich, C., Krug, K., Schütz, W., Jung, S., Nordheim, A., Sommer, R. J. and Macek, B. (2010). Proteogenomics of Pristionchus pacificus reveals distinct proteome structure of nematode models. *Genome Res.* **20**, 837-846.

Bos, J. L., Rehmann, H. and Wittinghofer, A. (2007). GEFs and GAPs: critical elements in the control of small g proteins. *Cell* **130**, 385.

Braun, A. C. and Olayioye, M. A. (2015). Rho regulation: DLC proteins in space and time. *Cell. Signal.* **27**, 1643-1651.

Braun, A. C., Hendrick, J., Eisler, S. A., Schmid, S., Hausser, A. and Olayioye, M. A. (2015). The Rho-specific GAP protein DLC3 coordinates endocytic membrane trafficking. *J. Cell Sci.* **128**, 1386-1399.

Bryant, D. M., Kerr, M. C., Hammond, L. A., Joseph, S. R., Mostov, K. E., Teasdale, R. D. and Stow, J. L. (2007). EGF induces macropinocytosis and SNX1-modulated recycling of E-cadherin. *J. Cell Sci.* **120**, 1818-1828.

Bryant, D. M., Datta, A., Rodríguez-Fraticelli, A. E., Peränen, J., Martín-Belmonte, F. and Mostov, K. E. (2010). A molecular network for de novo generation of the apical surface and lumen. *Nat. Cell Biol.* **12**, 1035-1045.

Chatterjee, S., Seifried, L., Feigin, M. E., Gibbons, D. L., Scuoppo, C., Lin, W., Rizvi, Z. H., Lind, E., Dissanayake, D., Kurie, J. et al. (2012). Dysregulation of cell polarity proteins synergize with oncogenes or the microenvironment to induce invasive behavior in epithelial cells. *PLoS ONE* **7**, e34343.

Courbard, J.-R., Djiane, A., Wu, J. and Mlodzik, M. (2009). The Apical/Basal-polarity determinant Scribble cooperates with the PCP core factor Stbm/Vang and functions as one of its effectors. *Dev. Biol.* **333**, 67-77.

Cox, J. and Mann, M. (2008). MaxQuant enables high peptide identification rates, individualized p.p.b.-range mass accuracies and proteome-wide protein quantification. *Nat. Biotechnol.* **26**, 1367-1372.

Cox, J., Neuhauser, N., Michalski, A., Scheltema, R. A., Olsen, J. V. and Mann, M. (2011). Andromeda: a peptide search engine integrated into the maxquant environment. *J. Proteome Res.* **10**, 1794-1805.

de Vreede, G., Schoenfeld, J. D., Windler, S. L., Morrison, H., Lu, H. and Bilder, D. (2014). The Scribble module regulates retromer-dependent endocytic trafficking during epithelial polarization. *Development* **141**, 2796-2802.

Dow, L. E., Brumby, A. M., Muratore, R., Coombe, M. L., Sedelies, K. A., Trapani, J. A., Russell, S. M., Richardson, H. E. and Humbert, P. O. (2003). hScrib is a functional homologue of the Drosophila tumour suppressor Scribble. *Oncogene* **22**, 9225-9230.

Dow, L. E., Kauffman, J. S., Caddy, J., Peterson, A. S., Jane, S. M., Russell, S. M. and Humbert, P. O. (2006). The tumour-suppressor Scribble dictates cell polarity during directed epithelial migration: regulation of Rho GTPase recruitment to the leading edge. *Oncogene* **26**, 2272-2282.

Dow, L. E., Elsum, I. A., King, C. L., Kinross, K. M., Richardson, H. E. and Humbert, P. O. (2008). Loss of human Scribble cooperates with H-Ras to promote cell invasion through deregulation of MAPK signalling. *Oncogene* **27**, 5988-6001.

Durkin, M. E., Ullmannova, V., Guan, M. and Popescu, N. C. (2007a). Deleted in liver cancer 3 (DLC-3), a novel Rho GTPase-activating protein, is downregulated in cancer and inhibits tumor cell growth. *Oncogene* **26**, 4580-4589.

Durkin, M. E., Yuan, B.-Z., Zhou, X., Zimonjic, D. B., Lowy, D. R., Thorgeirsson, S. S. and Popescu, N. C. (2007b). DLC-1:a Rho GTPase-activating protein and tumour suppressor. *J. Cell. Mol. Med.* **11**, 1185-1207.

Ellenbroek, S. I. J., Iden, S. and Collard, J. G. (2012). Cell polarity proteins and cancer. *Semin. Cancer Biol.* **22**, 208-215.

Elsum, I. A. and Humbert, P. O. (2013). Localization, not important in all tumor-suppressing properties: a lesson learnt from scribble. *Cells Tissues Organs* **198**, 1-11.

Erlmann, P., Schmid, S., Horenkamp, F. A., Geyer, M., Pomorski, T. G. and Olayioye, M. A. (2009). DLC1 activation requires lipid Interaction through a polybasic region preceding the RhoGAP domain. *Mol. Biol. Cell* **20**, 4400-4411.

Feigin, M. E., Akshinthala, S. D., Araki, K., Rosenberg, A. Z., Muthuswamy, L. B., Martin, B., Lehmann, B. D., Berman, H. K., Pietenpol, J. A., Cardiff, R. D. et al. (2014). Mislocalization of the cell polarity protein scribble promotes mammary tumorigenesis and is associated with basal breast cancer. *Cancer Res.* **74**, 3180-3194.

Frank, S. R., Bell, J. H., Frödin, M. and Hansen, S. H. (2012). A βPIX-PAK2 complex confers protection against Scrib-dependent and cadherin-mediated apoptosis. *Curr. Biol.* **22**, 1747-1754.

Gardiol, D., Zacchi, A., Petrera, F., Stanta, G. and Banks, L. (2006). Human discs large and scrib are localized at the same regions in colon mucosa and changes in their expression patterns are correlated with loss of tissue architecture during malignant progression. *Int. J. Cancer* **119**, 1285-1290.

Halaoui, R. and McCaffrey, L. (2015). Rewiring cell polarity signaling in cancer. *Oncogene* **34**, 939-950.

Holeiter, G., Bischoff, A., Braun, A. C., Huck, B., Erlmann, P., Schmid, S., Herr, R., Brummer, T. and Olayioye, M. A. (2012). The RhoGAP protein deleted in liver cancer 3 (DLC3) is essential for adherens junctions integrity. *Oncogenesis* **1**, e13.

Humbert, P. O., Grzeschik, N. A., Brumby, A. M., Galea, R., Elsum, I. and Richardson, H. E. (2008). Control of tumourigenesis by the Scribble/Dlg/Lgl polarity module. *Oncogene* **27**, 6888-6907.

Iden, S. and Collard, J. G. (2008). Crosstalk between small GTPases and polarity proteins in cell polarization. *Nat. Rev. Mol. Cell Biol.* **9**, 846-859.

Jaffe, A. B. and Hall, A. (2005). RHO GTPASES: biochemistry and biology. *Annu. Rev. Cell Dev. Biol.* **21**, 247-269.

Kawai, K., Kiyota, M., Seike, J., Deki, Y. and Yagisawa, H. (2007). START-GAP3/DLC3 is a GAP for RhoA and Cdc42 and is localized in focal adhesions regulating cell morphology. *Biochem. Biophys. Res. Commun.* **364**, 783-789.

Li, G., Du, X., Vass, W. C., Papageorge, A. G., Lowy, D. R. and Qian, X. (2011). Full activity of the deleted in liver cancer 1 (DLC1) tumor suppressor depends on an LD-like motif that binds talin and focal adhesion kinase (FAK). *Proc. Natl. Acad. Sci. USA* **108**, 17129-17134.

Lohia, M., Qin, Y. and Macara, I. G. (2012). The scribble polarity protein stabilizes E-cadherin/p120-catenin binding and blocks retrieval of E-cadherin to the golgi. *PLoS ONE* **7**, e51130.

Mack, N. A. and Georgiou, M. (2014). The interdependence of the Rho GTPases and apicobasal cell polarity. *Small GTPases* **5**, e973768.

Mack, N. A., Porter, A. P., Whalley, H. J., Schwarz, J. P., Jones, R. C., Khaja, A. S., Bjartell, A., Anderson, K. I. and Malliri, A. (2012). β2-syntrophin and Par-3 promote an apicobasal Rac activity gradient at cell-cell junctions by differentially regulating Tiam1 activity. *Nat. Cell Biol.* **14**, 1169-1180.

Mertens, A. E. E., Rygiel, T. P., Olivo, C., van der Kammen, R. and Collard, J. G. (2005). The Rac activator Tiam1 controls tight junction biogenesis in keratinocytes through binding to and activation of the Par polarity complex. *J. Cell Biol.* **170**, 1029-1037.

Möller, Y., Siegemund, M., Beyes, S., Herr, R., Lecis, D., Delia, D., Kontermann, R., Brummer, T., Pfizenmaier, K. and Olayioye, M. A. (2014). EGFR-targeted TRAIL and a smac mimetic synergize to overcome apoptosis resistance in KRAS mutant colorectal cancer cells. *PLoS ONE* **9**, e107165.

Montcouquiol, M., Rachel, R. A., Lanford, P. J., Copeland, N. G., Jenkins, N. A. and Kelley, M. W. (2003). Identification of Vangl2 and Scrb1 as planar polarity genes in mammals. *Nature* **423**, 173-177.

Murdoch, J. N., Henderson, D. J., Doudney, K., Gaston-Massuet, C., Phillips, H. M., Paternotte, C., Arkell, R., Stanier, P. and Copp, A. J. (2003). Disruption of scribble (Scrb1) causes severe neural tube defects in the circletail mouse. *Hum. Mol. Genet.* **12**, 87-98.

Navarro, C., Nola, S., Audebert, S., Santoni, M.-J., Arsanto, J.-P., Ginestier, C., Marchetto, S., Jacquemier, J., Isnardon, D., Le Bivic, A. et al. (2005). Junctional recruitment of mammalian Scribble relies on E-cadherin engagement. *Oncogene* **24**, 4330-4339.

Ngok, S. P., Lin, W.-H. and Anastasiadis, P. Z. (2014). Establishment of epithelial polarity – GEF who's minding the GAP? *J. Cell Sci.* **127**, 3205-3215.

Nishimura, T., Yamaguchi, T., Kato, K., Yoshizawa, M., Nabeshima, Y.-I., Ohno, S., Hoshino, M. and Kaibuchi, K. (2005). PAR-6-PAR-3 mediates Cdc42-induced Rac activation through the Rac GEFs STEF/Tiam1. *Nat. Cell Biol.* **7**, 270-277.

Nola, S., Sebbagh, M., Marchetto, S., Osmani, N., Nourry, C., Audebert, S., Navarro, C., Rachel, R., Montcouquiol, M., Sans, N. et al. (2008). Scrib regulates PAK activity during the cell migration process. *Hum. Mol. Genet.* **17**, 3552-3565.

Noren, N. K., Arthur, W. T. and Burridge, K. (2003). Cadherin engagement inhibits RhoA via p190RhoGAP. *J. Biol. Chem.* **278**, 13615-13618.

Nourry, C., Grant, S. G. N. and Borg, J.-P. (2003). PDZ domain proteins: plug and play! *Sci. Signal.* **2003**, re7.

Pagliarini, R. A. and Xu, T. (2003). A genetic screen in drosophila for metastatic behavior. *Science* **302**, 1227-1231.

Piekny, A. J. and Glotzer, M. (2008). Anillin is a scaffold protein that links RhoA, actin, and myosin during cytokinesis. *Curr. Biol.* **18**, 30-36.

Priya, R., Gomez, G. A., Budnar, S., Verma, S., Cox, H. L., Hamilton, N. A. and Yap, A. S. (2015). Feedback regulation through myosin II confers robustness on RhoA signalling at E-cadherin junctions. *Nat. Cell Biol.* **17**, 1282-1293.

Qian, X., Li, G., Asmussen, H. K., Asnaghi, L., Vass, W. C., Braverman, R., Yamada, K. M., Popescu, N. C., Papageorge, A. G. and Lowy, D. R. (2007). Oncogenic inhibition by a deleted in liver cancer gene requires cooperation between tensin binding and Rho-specific GTPase-activating protein activities. *Proc. Natl. Acad. Sci. USA* **104**, 9012-9017.

Qin, Y., Capaldo, C., Gumbiner, B. M. and Macara, I. G. (2005). The mammalian Scribble polarity protein regulates epithelial cell adhesion and migration through E-cadherin. *J. Cell Biol.* **171**, 1061-1071.

Ratheesh, A., Gomez, G. A., Priya, R., Verma, S., Kovacs, E. M., Jiang, K., Brown, N. H., Akhmanova, A., Stehbens, S. J. and Yap, A. S. (2012). Centralspindlin and α-catenin regulate Rho signalling at the epithelial zonula adherens. *Nat. Cell Biol.* **14**, 818-828.

Röring, M., Herr, R., Fiala, G. J., Heilmann, K., Braun, S., Eisenhardt, A. E., Halbach, S., Capper, D., von Deimling, A., Schamel, W. W. et al. (2012). Distinct requirement for an intact dimer interface in wild-type, V600E and kinase-dead B-Raf signalling. *EMBO J.* **31**, 2629-2647.

Schwanhäusser, B., Busse, D., Li, N., Dittmar, G., Schuchhardt, J., Wolf, J., Chen, W. and Selbach, M. (2011). Global quantification of mammalian gene expression control. *Nature* **473**, 337-342.

Terry, S. J., Zihni, C., Elbediwy, A., Vitiello, E., Leefa Chong San, I. V., Balda, M. S. and Matter, K. (2011). Spatially restricted activation of RhoA signalling at epithelial junctions by p114RhoGEF drives junction formation and morphogenesis. *Nat. Cell Biol.* **13**, 159-166.

Tripathi, V., Popescu, N. C. and Zimonjic, D. B. (2012). DLC1 interaction with α-catenin stabilizes adherens junctions and enhances DLC1 antioncogenic activity. *Mol. Cell. Biol.* **32**, 2145-2159.

Vigil, D., Cherfils, J., Rossman, K. L. and Der, C. J. (2010). Ras superfamily GEFs and GAPs: validated and tractable targets for cancer therapy? *Nat. Rev. Cancer* **10**, 842-857.

Vitiello, E., Ferreira, J. G., Maiato, H., Balda, M. S. and Matter, K. (2014). The tumour suppressor DLC2 ensures mitotic fidelity by coordinating spindle positioning and cell–cell adhesion. *Nat. Commun.* **5**, 5826.

Wildenberg, G. A., Dohn, M. R., Carnahan, R. H., Davis, M. A., Lobdell, N. A., Settleman, J. and Reynolds, A. B. (2006). p120-catenin and p190RhoGAP regulate cell-cell adhesion by coordinating antagonism between Rac and Rho. *Cell* **127**, 1027-1039.

Yamada, S. and Nelson, W. J. (2007). Localized zones of Rho and Rac activities drive initiation and expansion of epithelial cell–cell adhesion. *J. Cell Biol.* **178**, 517-527.

Zeitler, J., Hsu, C. P., Dionne, H. and Bilder, D. (2004). Domains controlling cell polarity and proliferation in the Drosophila tumor suppressor Scribble. *J. Cell Biol.* **167**, 1137-1146.

Zhan, L., Rosenberg, A., Bergami, K. C., Yu, M., Xuan, Z., Jaffe, A. B., Allred, C. and Muthuswamy, S. K. (2008). Deregulation of Scribble promotes mammary tumorigenesis and reveals a role for cell polarity in carcinoma. *Cell* **135**, 865-878.